

Ultrasound Image Segmentation based on the Mean-Shift and Graph Cuts Theory

^{1,2}Ting Yun and ^{1,2}Yiqing Xu

¹Department of Computer Science, Southeast University, Nanjing, 210096, China

²Department of Information and Science, Nanjing Forestry University, Nanjing, 210027, China

Abstract: This study addressed the issue of vascular ultrasound image segmentation and proposed a novel ultrasonic vascular location and detection method. We contributed in several aspects: Firstly using mean-shift segmentation algorithm to obtain the initial segmentation results of vascular images; Secondly new data item and smooth item of the graph cut energy function was constructed based on the MRF mode, then we put forward swap and α expansion ideas to optimize segmentation results, consequently accurately located the vessel wall and lumen in vascular images. Finally comparison with experts manually tagging results and Applying edge correlation coefficients and variance to verify the validity of our algorithm, experimental results show that our algorithm can efficiently combines the advantages of mean-shift and graph-cut algorithm and achieve better segmentation results.

Keywords: Gauss mixture model, graph-cut algorithm, mean-shift, ultrasound image

INTRODUCTION

Medical ultrasound image is an important type of medical images and is widely used in medical diagnosis, Compared with other medical imaging methods, ultrasound imaging has the advantages of nonease to use. As an ideal non-invasive diagnosis method-traumatic to human body, real-time display, low for human eyes observation or machine analysis, in recent years for ultrasound images automatic pathological area segmentation algorithm become the research focus, some scholars dealt with the ultrasound image cost, it has broad prospects for development. However, due to the constraints of the ultrasound imaging principle, it leads to insufficient grayscale display range and unreasonable gray distribution, so the ultrasound images auxiliary diagnosis effect is limited, especially in some local details. That will bring a lot of difficult to detect if gray level difference of pathological regions are not obvious. In order to improve ultrasound images quality and enhance the local details readability in ultrasound image, make images suitable segmentation in the frequency domain, such as İşcan and Kurnaz (2006) used wavelet decomposition to achieve wavelet coefficients, then combined with neural network method to process segmentation problem. Yan *et al.* (2010) constructed an accurate ultrasound image segmentation algorithm in the wavelet domain with the Chan-Vese model, (Kermani and Ayatollahi, 2010) combined the local histogram and wavelet transform to locate the position of breast lesions in ultrasound image. Xie *et al.* (2005)

proposed a new method which took texture and shape as the prior information, then constructed energy equation and classified texture of pathological area by the shape parameter and Gabor filter coefficients. Other researchers processed ultrasound image in the space domain, (Cardinal *et al.*, 2006) proposed segmentation algorithm based on gray probability density function and fast matching learning ideas for vascular images, (Grady and Funka-Lea, 2004) constructed an image segmentation method based on graph theory, which has the advantages of robust to noise, sensitive to the blurred edge, low residual error rate and fast calculation speed. After remove speckle noise, (Cremers *et al.*, 2007; Dydenko *et al.*, 2005; Sarti *et al.*, 2005) adopted active contour model combining with prior information such as shape, texture, color, etc., to complete pathology region extraction. Christodoulou and Pattichis (2003) used ten different texture feature include first-order statistics, gray-level co-occurrence matrix, gray differential statistics, neighborhood gray difference matrix, statistical feature matrix, texture energy spectrum, characteristic of fractal dimension, power spectrum and shape parameters to extract carotid atherosclerotic plaques, then combined K-neighboring method to get the result.

Due to the ultrasound imaging mechanism is complex, characteristics of pathological regions are disturbed by noise and un-pathological regions, so the visual features of critical regions are not distinct, the swap thought of graph cut algorithm can only get local optimum solution, so for the excessive interference ultrasound image cannot achieve satisfactory results, if

increase the iteration steps that will spend more time, thus vascular ultrasound image segmentation method based on mean-shift and graph cut theory was proposed in this study. Firstly mean-shift method was adopted for initial vascular ultrasound image segmentation, through mean-shift algorithm iteration to the ultrasound image, small adjacent areas with similar gray attribute were classified into one class; Secondly a new data and smooth item of the energy function was defined and the graph cut method was used to obtain the global optimal solution, thereby optimization and correction of segmentation results were realized, then the vessel wall edge and vessel lumen were accurately located; Finally comparing with the manual tagging results the validity of our algorithm was proved.

MEAN-SHIFT ULTRASOUND IMAGE SEGMENTATION METHOD

Mean-shift computational method is an effective tool for analysis in feature space, it has widely used in many computer vision applications. Mean-shift is an algorithm with no parameters estimation and its main function is a probability density gradient function, it along the gradient rising direction to find the peak of the probability distribution. As the kernel density estimation, kernel function generally meets the conditions: $K(p) = c_{k,d} (\|p\|^2)$, where, $K(p)$ ($p \geq 0$) called kernel function and p represents single pixel in the image domain, the normalization positive constant $c_{k,d}$ is to ensure that integral of $K(p)$ equal to 1. In mean-shift method Gaussian kernel function and uniform kernel function is two kind of commonly used kernel function, let $g(p) = -K(p)$, kernel function $G(p)$ define $G(p) = c_{g,d} g(\|p\|^2)$ and mean shift vector is defined as formula (1):

$$m_{h,k}(p) = \frac{\sum_{i=1}^n p_i g(\|(p-h-p_i)/h\|^2)}{\sum_{i=1}^n g(\|(p-p_i)/h\|^2)} - x \quad (1)$$

p_i is the sample point of the current Parzen window. Mean-shift solving steps include two parts:

- Calculation mean shift vector $m_{h,k}(p)$
- According to the $m_{h,k}(p)$ value to transform nuclear location

The second process ensures to converge to the points which neighborhoods' gradient is zero. Let $\{y_j\}$ $j = 1, 2, \dots, n$ is the nuclear location sequence during mean-shift process, by the formula (1) can be got:

$$y_{i,j+1} = \frac{\sum_{i=1}^n p_i g(\|(p-p_i)/h\|^2)}{\sum_{i=1}^n g(\|(p-p_i)/h\|^2)}, j=1,2,\dots \quad (2)$$

Formula (2) calculates weight mean value with kernel function G in $y_{i,j}$ position, where $y_{i,1}$ is the initial position of kernel.

Ultrasound image segmentation method based on mean-shift algorithm can be described as: Firstly, the ultrasonic image can be represented as a two-dimensional grid in three-dimensional space, grid space is called spatial domain, gray value space also called range domain. Through searching for the next shift point in the image space and set the stop conditions, until the displacement value is less than a given value, then iteration is stopped.

Let x_i represents the input vector and z_i ($i = 1, 2, \dots, n$) represents the filter output results. For the all data points x_i $i = 1, 2, \dots, n$, mean-shift vector $m_{h,k}(x)$ of each point are calculated, according to the $m_{h,k}(x)$ value that moving window center shift to the next point, this process is repeated until convergence to the density peak of the data space, when the estimated density gradient is zero, then no need to move and assign the pixel value P_x to z_i , that is $z_i = P_x$. z_i is the filtered pixel. The output image consists of multiple independent regions. Basic steps are as follows:

- Initialize $j = 1$ and $y_{i1} = x_i$
- According to Eq. (2), calculate $y_{i,j+1}$ until convergence and record convergence value is $y_{i,c}$
- Assign $z_i = (x_{is}, y_{i,c}^r)$

Through the above three steps we can get final results of mean-shift filter, where superscript s and subscript r respectively represent spatial domain and value range. Using mean-shift filtering method, need to set bandwidth vector $h = (h_s, h_r)$. Bandwidth can be regarded as the resolution of segmentation, bandwidth is larger, more details of the image will be ignored, how to choose the appropriate bandwidth, is the key of successfully using kernel density function. In this study radial gauss kernel function is adopted for ultrasound image segmentation.

ULTRASOUND IMAGE SEGMENTATION OPTIMIZATION BASED ON THE GRAPH CUT THEORY

Graph cut algorithm is a global optimization algorithm, by using the class label and constructing energy function, it convert image segmentation problem into the energy function minimizing problem. Under the guidance of the graph cut theory, network is ingeniously constructed and energy is linked to the network capacity, at last network flow principle about graph theory is adopted to find the graph minimum cut, the cut is optimal solution of the energy function minimization problem, besides the image segmentation is completed. Graph cut algorithm are two thoughts, include *swap* and *α expansion*. But at first we construct graph cut energy function based on the MRF model.

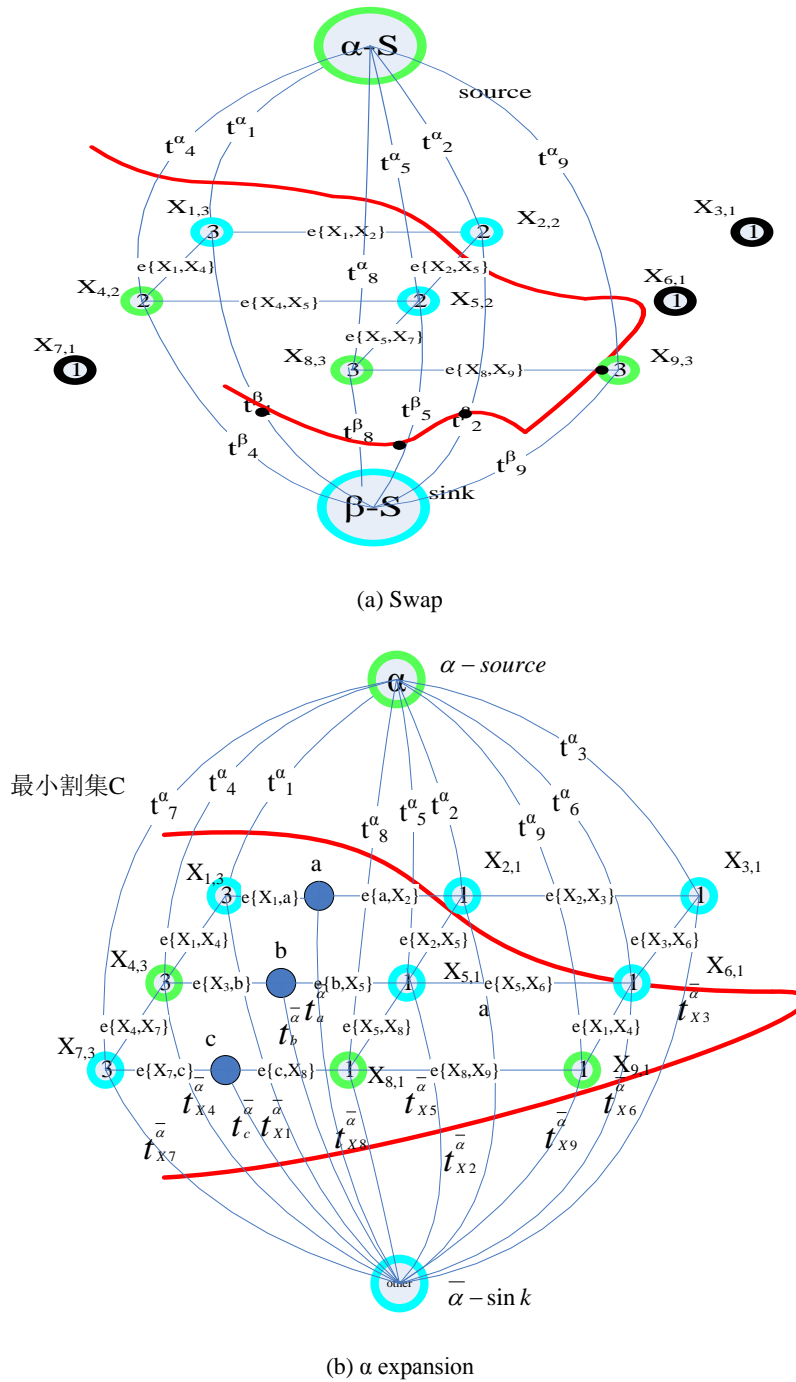


Fig. 1: Graph cut algorithm principle diagram

Ultrasound image segmentation model based on MRF: Image segmentation approach based on the MRF model can be seen as optimization problems, that are acquisition the label field f which make energy function $E(f)$ minimization. We constructed energy function expressed as follows:

$$E(f) = E_{smooth}(f) + E_{data}(f) = \sum_{\{p,q\} \in N} V_{p,q}(f_p, f_q) + \sum_{p \in P} D_p(f_p, w_i) \quad (3)$$

where, $E_{smooth}(f)$ called smooth item, it is the punishment to the un-smoothness characteristics; $E_{data}(f)$ known as the data item energy, it is the punishment to the disagreement between current class label f and observation data w_i class. For a given image, p represent each pixel, P is the set of all pixels, all neighboring pixel pair $\{p, q\}$ that constitute the set N . Where $V_{p, q}(f_p, f_q)$ uses four neighborhood Potts model (Fjortoft *et al.*, 2003): $E_{smooth} = (f) = V_{p, q}(f_p,$

$f_q) = \lambda \delta (f_p \neq f_q)$, λ is the factor to balance the data item and smoothing item, each pixel data item energy $D_p (f_p)$ in type (3) can be got by type (4):

$$D_p (f_p, w_i) = \hat{f}_{w_i} (y_p) = \frac{1}{\sqrt{2\pi\sigma_i}} \exp\left(-\frac{1}{2}\left(\frac{\delta_p - \mu_i}{h}\right)^2\right) \quad (4)$$

where,

δ_p : Attribute value of pixel p (such as gray value)
 $\hat{f}_{w_i} (\delta_p)$: The probability of pixel p belongs to the category w_i

We used the mean-shift method to obtain the initial ultrasound image segmentation and got mean values and variances of w classes:

$\theta = (\mu_1, \mu_2, \dots, \mu_w, \sigma_1, \sigma_2, \dots, \sigma_w)$, with gauss RBF kernel function (4) gets likelihood estimation of the pixel p to the corresponding w classes. Where h control the smoothness range of function (4), when the value of h is large, function curve is more smooth, but may lose more detail information; when the value of h is smaller, function curve will be more sharper, that will over-reliance on the observation data, then the algorithm performance will degrade. In Cardinal *et al.* (2006): the method to estimation h is given, such as:

$$h = \mu \exp\left(\frac{\alpha}{n} - frq(\delta)\gamma\right)$$

where,

$frq(\delta)$: The occurrence frequency of y in the training sample set

Graph-cut algorithm: swap algorithm ideas: The swap algorithm of graph cut is repeatedly calculation two different categories w_α, w_β and in order to obtain the optimal solution of equation, the graph grid is constructed to associate with energy Eq. (3). Let P is the set of all pixels, while $P_{\alpha\beta}$ is a pixel points set which class belong to w_α, w_β , grid construction as shown in Fig. 1(a), the elements in Fig. 1(a) are: vertex set $V = \{\alpha - S, \beta - S, P\}$, edge set:

$$\mathcal{E} = \left\{ \bigcup_{p \in P} \{t_p^\alpha, t_p^\beta\}, \bigcup_{\{p,q\} \in N} e_{\{p,q\}} \right\}$$

where, $\alpha - S, \beta - S$ is two graph vertex, $P = \{p|p = 1, 2, 3, \dots, 12\}$, $X_{p,\alpha}$ in Fig. 1(a) represent pixel p belong to the class w_α through mean-shift method calculation. Pixel p (satisfy $f_p = \alpha$ or $f_p = \beta$) in $P_{\alpha\beta}$ respectively connect with two vertices $\alpha - S, \beta - S$ that constitute t-link edges, denoted by t_p^α, t_p^β and the elements among $P_{\alpha\beta}$ constitute n-link edges between each other, denoted

by $e_{\{p,q\}}$, the weight of t-link and n-link assignment approach respectively see Eq. (5) and (6):

$$t_p^\alpha = D_p (f_p, w_\alpha) + \sum_{\substack{q \in N_p \\ q \in P_{\alpha\beta}}} V(w_\alpha, f_q) \quad p \in P_{\alpha\beta} \quad (5)$$

$$t_p^\beta = D_p (f_p, w_\beta) + \sum_{\substack{q \in N_p \\ q \in P_{\alpha\beta}}} V(w_\beta, f_q) \quad p \in P_{\alpha\beta}$$

$$e_{\{p,q\}} = V(f_p, f_q) \quad \{p,q\} \in N \quad p,q \in P_{\alpha\beta} \quad (6)$$

where, N_p is adjacent area of pixel p, (Szeliski *et al.*, 2008) prove the capacity of cut set is: $|C| = E - K$ (7). Where E is the energy value of Eq. (3), K is a constant, the optimal solution of energy function (3) is the minimal cut set of Fig. 1(a). Swap algorithm randomly select two classes w_α, w_β from w class and through the energy function to calculate the corresponding cut set, then determine all pixels belong to which class, thus get the optimal segmentation results, specifically shown in Fig. 1(a).

Graph-cut algorithm:

α expansion algorithm ideas: The swap algorithm can only by means of exchange w_α, w_β class to calculate of the minimum energy. If we limit w_β and make w_α exchange with all other classes, then will get a broader transformation approach, it is α expansion algorithm. Boykov *et al.* (2001) proved when formations of smooth item satisfy ‘metrics’ constrain, then α expansion algorithm ideas can be adopted to achieve more broader transformation, as shown in Fig. 1(b), a set of vertices V :

$$V = \left\{ \alpha - source, \bar{\alpha} - \sin k, P, \bigcup_{\substack{\{p,q\} \in N \\ f_p \neq f_q}} Z_{\{p,q\}} \right\}$$

is the composition elements of the graph, where $\alpha - source, \bar{\alpha} - \sin k$ respectively the highest and lowest vertices. p is the any pixel in P, q is adjacent pixels of p, $q \in N$. When the two pixel class label f_p and f_q are unequal, then auxiliary nodes $Z_{\{p,q\}}$ are added, Let $a, b, c \in Z_{\{p,q\}}$ are the auxiliary node, adding the auxiliary node $a(X_{1,3}, X_{2,1})$ between $X_{1,3}$ and $X_{2,1}$, as shown in Fig. 1(b), similarly, there are auxiliary nodes b ($X_{4,3}, X_{5,1}$) and c ($X_{7,3}, X_{8,1}$). Where edge set is:

$$\mathcal{E} = \left\{ \bigcup_{p \in P} \{t_p^\alpha, t_p^{\bar{\alpha}}\}, \bigcup_{\substack{\{p,q\} \in N \\ disp(p)=disp(q)}} e_{\{p,q\}}, \bigcup_{\substack{\{p,q\} \in N \\ disp(p) \neq disp(q)}} \xi_{\{p,q\}} \right\}$$

$\xi_{\{p,q\}}$ are the edges that between auxiliary node $Z_{\{p,q\}}$ with nodes p, q, $\bar{\alpha}$. For example Fig. 1(b) shows that

total three edges of c , the edge $e_{\{X73, c\}}$ between c and $X73$, the edge $e_{\{c, X81\}}$ between c and $X81$; the edge $t_c^{\bar{\alpha}}$ between c and $\bar{\alpha}$, similarly, auxiliary node a and b construct edges with their adjacent nodes. the pixels of P respectively connected with α and $\bar{\alpha}$ to construct t-link edges, the pixels among P connect with each other to constitute n-link edges, assignment edge weights method is expressed by formula (7) and (8), if existing auxiliary node c , then the edge weight between c and adjacent points can refer to the following formula (9):

$$\begin{aligned} t_p^{\bar{\alpha}} &= \infty \quad p \in P_\alpha \\ t_p^{\bar{\alpha}} &= D_p(f_p, w_\alpha) \quad p \notin w_\alpha, p \in w_i \\ t_p^\alpha &= D_p(f_p, w_\alpha) \quad p \in P_\alpha \end{aligned} \quad (7)$$

$$e_{\{p,q\}} = V(f_p, w_\alpha) \quad \{p, q\} \in N, f_p = f_q \quad (8)$$

$$\begin{aligned} e_{\{p,c\}} &= V(f_p, w_\alpha) \{p, q\} \in N, f_p \neq f_q \\ e_{\{c,q\}} &= V(w_\alpha, f_q) \{p, q\} \in N, f_p \neq f_q \\ t_c^{\bar{\alpha}} &= V(f_p, f_q) \{p, q\} \in N, f_p \neq f_q \end{aligned} \quad (9)$$

where, the definition of data item D see formula (4), smooth item V as shown in formula (3). Boykov *et al.* (2001) proved that the cut-set capacity is $|C| = E$ (11), where E is obtained from Eq. (3), then using the method of α expansion to optimally solve the Eq. (11). The steps of α expansion algorithm is: construct the network shown in Fig. 1(b), pixel set P ; Label set is the same definition as *swap* algorithm, for the classes of the P , if the pixel labels are α and $\bar{\alpha}$, then set t-link and n-link edges to find the minimum graph cut set C , equivalent to seek the minimum energy E' which corresponding to the class label L' , if condition $E' < E$ is satisfied, then modify the class label by the same mode of *swap* algorithm and update the class set of every pixel to L' . If $E' > E$, then exchange $\bar{\alpha}$ to other class and calculate the energy until $E' < E$.

EXPERIMENTAL RESULTS

The experiment of four ultrasound images is shown in Fig. 2.

Then variance and correlation coefficients are used for comparison of test results, variance represents deviation degree of the two boundary points, while the correlation coefficients indicate similarity of two boundary shape.

Firstly starting positions in the two boundaries are chose, then two L sub-sequence (R_1 and R_2) with fixed length in two curves are taken, The similarity of R_1 and R_2 notes for $\text{simil}_L(R_1, R_2)$, it depicts by $R_1 - R_2$

variance, that is $\text{simil}_L(R_1, R_2) = \text{SE}_L(R_1, R_2)$, where variance $\text{SE}_L(R_1 - R_2) = \frac{1}{L} \sum_{i=1}^L [(R_{1i} - R_{2i}) - \text{mean}]^2 / L$
 $\text{mean} = \sum_{i=1}^L (R_{1i} - R_{2i}) / L$, SE_L is smaller, the R_1 and R_2 are more similar, where R_{1i} represents the distance between sampling points on a curve to the origin. Correlation coefficients ρ_L are adopted for edge comparison. $\rho_L = \frac{\text{Cov}(R_1, R_2)}{\delta_1 \delta_2}$, $\text{Cov}(R_1, R_2)$ represents covariance between curve R_1 and curve R_2 , δ_1 and δ_2 respectively denote the standard deviation of R_1 and R_2 :

$$\text{Cov}(R_1, R_2) = \frac{1}{n} \sum_{i=1}^n (R_{1i} - \bar{R}_1)(R_{2i} - \bar{R}_2) \quad (10)$$

$$\delta_1 = \sqrt{\frac{1}{n} \sum_{i=1}^n (R_{1i} - \bar{R}_1)^2}, \quad \delta_2 = \sqrt{\frac{1}{n} \sum_{i=1}^n (R_{2i} - \bar{R}_2)^2}$$

\bar{R}_1 \bar{R}_2 represent the mean distance of all points on curves R_1 and R_2 to the origin.

Next, true positive ratio (True Positive ratio, TP), false-positive ratio (False Positive ratio, FP) and total similarity degree (Similarity, SI) are adopted, these three indicators evaluate the tumor region differences between the expert manual labeled results and our algorithm calibrates segmentation results (Madabhushi and Metaxas, 2003):

$$TP = \frac{|A_M \cap A_S|}{|A_M|}, \quad FP = \frac{|A_M \cup A_S - A_M|}{|A_M|}, \quad SI = \frac{|A_M \cap A_S|}{|A_M \cup A_S|} \quad (11)$$

where,

A_S : Tumor region of our algorithm segmentation

A_M : The doctors manually label tumor area

TP: Is higher, that our segmentation results cover the higher degree of expert manual calibration area

FP: Index is lower, then the covered wrong area is less

SI: Index is higher, that our segmentation result is closer to the manual label area

In this study we define:

$$TP = (TP_{\text{wall}} + TP_{\text{lumen}}) / 2, \quad FP = (FP_{\text{wall}} + FP_{\text{lumen}}) / 2$$

$$SI = (SI_{\text{wall}} + SI_{\text{lumen}}) / 2$$

Table 1 shows the specific experimental parameters and experimental results, including the selection threshold and the comparison between our algorithm and manual segmentation results, by calculating the correlation coefficients and variance of the curves to compare the similarity between them. From the experimental results can be seen, our designed

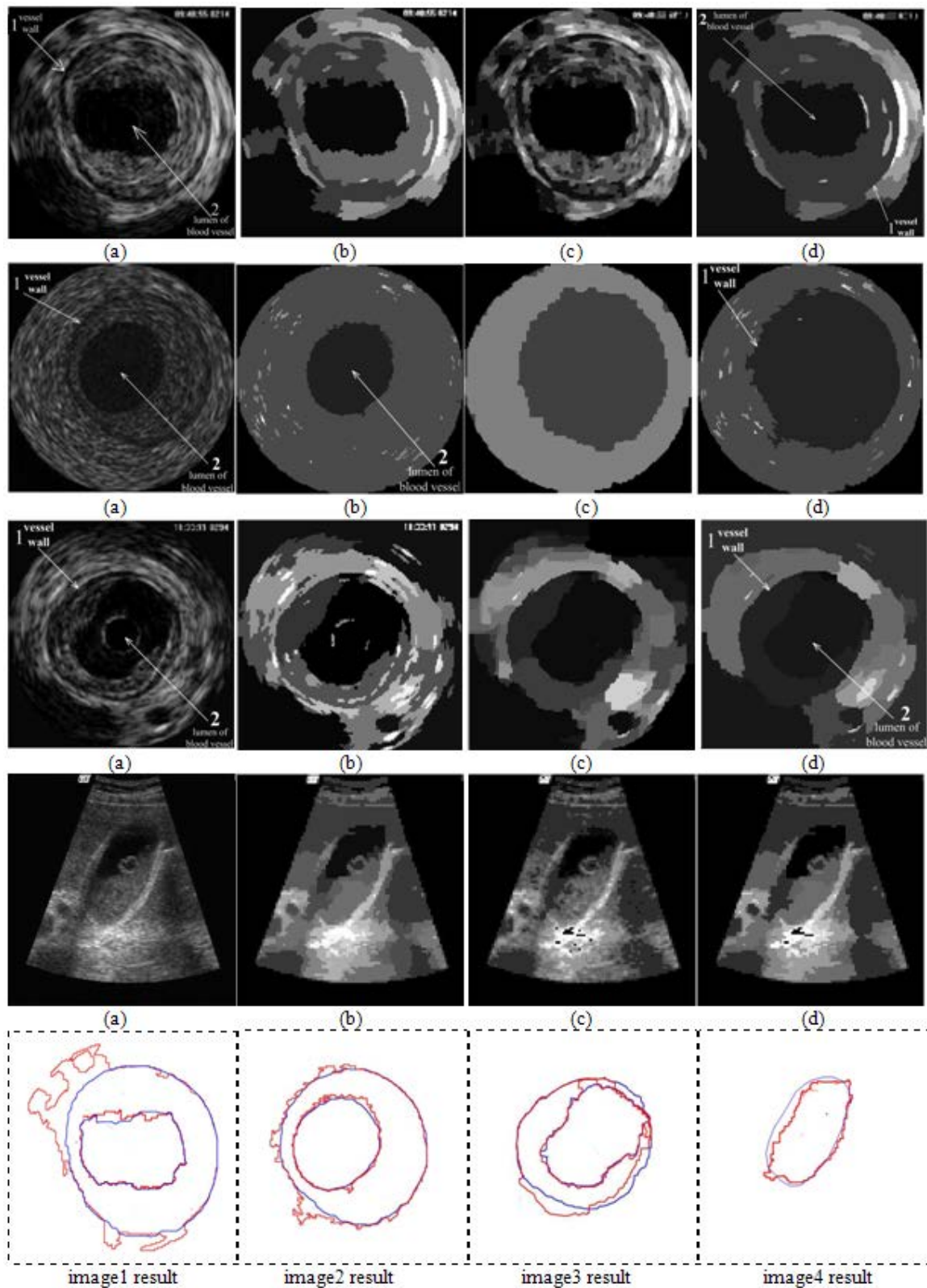


Fig. 2: Segmentation of ultrasound images, first columns (a) the original ultrasound images, second columns (b) three snapshot for only mean-shift segmentation results, third columns (c) only the graph cut algorithm used to get the segmentation results, fourth columns (d) segmentation of our algorithm, using graph cut re-segmentation after mean-shift segmentation results, where label 1 represents the vessel wall and label 2 represents lumen of blood vessel

Table 1: Selected coefficients and experimental results

	The h of equal (1)	The h of equal (4)	Vessel wall segmentation comparison with hand-labeling		Vessel lumen segmentation comparison with hand-labeling		TP (%) Wall + lumen	FP (%) Wall + lumen	SI (%) Wall + lumen
			Variance	Correlation coefficient	Variance	Correlation coefficient			
Ultrasound image 1	h = 17	60	25.7	0.7789	13.2	0.8524	92.1	22.07	77.92
Ultrasound image 2	h = 13	90	12.6	0.9121	8.4	0.9456	95.3	8.90	86.80
Ultrasound image 3	h = 13	90	21.2	0.7833	11.8	0.9219	89.6	17.21	80.31
Ultrasound image 4	h = 14	90			10.6	0.9019	87.6	9.50	79.44

algorithm can completely extract vascular lumen and accurately locate the position of the vessel wall, it has excellent performance in vascular ultrasound image segmentation.

The last row in Fig. 2 is comparison chart about above four ultrasound image segmentation results, blue lines represents the medical experts hand-labeled results of vessel cell and lumen edge, the red line is the labeling results of our algorithm.

CONCLUSION AND RECOMMENDATIONS

This study present a novel vascular ultrasound image segmentation method which combining mean-shift and graph cut algorithm, firstly mean-shift algorithm is adopted for the initial segmentation, then initial classification results which include specific characteristic parameters of each class are obtained according to the histogram classification, subsequently probabilistic model is used to construct data and smooth items of energy function and then we used graph cut method to get the optimal solution of the energy function, thereby locating the position of vessel wall and vessel lumen, comparison with expert manual segmentation results, our algorithm realize vascular localization function. Our future work mainly include two aspects, firstly how to accurately and effectively locate the ultrasound vascular image edge when acquisition ultrasound image visual quality are not well, secondly when the amount of medical image data is too large, how to improve calculation speed of maximum flow/ minimum cut algorithm and enhance the graph-cut real-time performance for better adapt for the segmentation of ultrasound images, these will be the focus of our future work.

ACKNOWLEDGMENT

The authors wish to thank the helpful comments and suggestions from my teachers and colleagues in medical imaging Lab of southeast University. This work is subsidized by the National Key Basic Research Program Project 973 (2011CB707904). High academic qualifications fund of Nanjing Forestry University (163070052 163070036).

REFERENCES

- Boykov, Y., O. Veksler and R. Zabih, 2001. Fast approximate energy minimization via graph cuts. *IEEE Trans. Patt. Anal.*, 33(3): 181-200.
- Cardinal, M.H., J. Meunier, G. R.L. Soulez Maurice, E. Therasse, *et al.*, 2006. Intravascular ultrasound image segmentation: A three-dimensional fast-marching method based on gray level distributions. *IEEE Trans. Med. Imag.*, 25(5): 590-602.
- Christodoulou, C.I. and C.S. Pattichis, 2003. Texture based classification of atherosclerotic carotid plaques. *IEEE Trans. Med. Imag.*, 22(7): 902-912.
- Cremers, D., M. Rousson and R. Deriche, 2007. A review of statistical approaches to level set segmentation: Integrating color, texture, motion and shape. *Int. J. Comp. Vision*, 72(2): 195-215.
- Dydenko, I., F. Jamal, O. Bernard, J. D'hooge, I.E. Magnin, *et al.*, 2005. A level set framework with a shape and motion prior for segmentation and region tracking in echocardiography. *Med. Image Anal.*, 10(2): 162-177.
- Fjortoft, R., Y. Delignon, W. Pieczynski, S. Marc and T. Florence, 2003. Unsupervised classification of radar images using hidden markov chains and hidden markov random fields. *IEEE Trans. Geosci. Remote Sens.*, 41(3): 675-686.
- Grady, L. and G. Funka-Lea, 2004. Multi-label image segmentation for medical applications based on graph-theoretic electrical potentials. *Proceedings of Conference on Computer Vision and Mathematical Methods in Medical and Biomedical Image Analysis*, pp: 230-245.
- İşcan, Z. and M.N. Kurnaz, 2006. Ultrasound image segmentation by using wavelet transform and self organizing neural network. *Neural Inform. Proc-Lett. Rev.*, 10(8): 183-190.
- Kermani, A. and A. Ayatollahi, 2010. Medical ultrasound image segmentation by modified local histogram range image method. *Biomed. Sci. Eng.*, 3: 1078-1084.
- Madabhushi, A. and D.N. Metaxas, 2003. Combining low-high-level and empirical domain knowledge for automated segmentation of ultrasonic breast lesions. *IEEE Trans. Med. Imag.*, 22(2): 155-169.

- Sarti, A., C. Corsi, E. Mazzini and C. Lamberti, 2005. Maximum likelihood segmentation of ultrasound images with Rayleigh distribution. *IEEE Trans. Ultrason. Ferroelect. Frequen. Cont.*, 52(6): 947-960.
- Szeliski, R., R. Zabini, D. Scharstein O. Veksler, V. Kolmogorov, *et al.*, 2008. A comparative study of energy minimization methods for markov random fields with smoothness-based priors. *IEEE Trans. Patt. Anal.*, 30(5): 1068-1080.
- Xie, J., Y. Jiang and H.T. Tsui, 2005. Segmentation of kidney from ultrasound images based on texture and shape priors. *IEEE Trans. Med. Imag.*, 24(1): 539-551.
- Yan, S., J.P. Yuan and C.H. Hou, 2010. Segmentation of medical ultrasound images based on level set method with edge representing mask. *Proceedings of 3rd International Conference on Advanced Computer Theory and Engineering*, pp: v2-85-v2-88.